Excitonic properties of zinc-blende ZnSe/MgS superlattices studied by reflection spectroscopy

Hidekazu Kumano
Department of Physics, Hokkaido University, Sapporo 060, Japan

Hiroyuki Nashiki, Ikuo Suemune,* Munetaka Arita, Toshio Obinata, Hideki Suzuki, and Katsuhiro Uesugi
Research Institute for Electronic Science, Hokkaido University, Sapporo 060, Japan

Jun'ichiro Nakahara
Department of Physics, Hokkaido University, Sapporo 060, Japan
(Received 18 April 1996; revised manuscript received 21 October 1996)

Excitonic properties of newly developed zinc-blende ZnSe/MgS superlattices (SL's) were measured by reflection spectroscopy. The modification of the excitonic peaks by the multiple reflection in the SL films was treated theoretically and a fitting method to estimate the exciton absorption peak positions and exciton linewidths was developed. Although zinc-blende MgS did not exist before, excellent optical properties were observed in the ZnSe/MgS SL's. Excitonic structures were clearly observed from 13 K up to the measured room temperature. In spite of strong ionicity of MgS barrier layers in the ZnSe/MgS SL's, the reduction of exciton–LO-phonon coupling was clearly observed in narrower wells. This indicates that the quantum confinement effect on excitons is large due to the large band offsets and it overcomes the enhancement of exciton–LO-phonon scattering due to high ionicity in barrier layers. [S0163-1829(97)03307-9]

I. INTRODUCTION

There has been a great deal of interest recently in wide-band-gap II-VI semiconductors because of its attraction for basic physics as well as their potential to realize blue/green light-emitting devices. Exciton binding energies are larger than those in III-V semiconductors mainly because of larger electron and hole effective masses, and further enhancement of excitonic effects is expected by introducing the quantum confinement in quantum well (QW) and superlattice (SL) structures. In blue/green range, $Zn_xCd_{1-x}Se/ZnS_xSe_{1-x}$ strained SL's have been primarily studied on their excitonic properties.[1–3] The band offsets are increased with higher Cd composition in the well layers. However, the strain induced with Cd incorporation limits the band offsets in these strained SL's. The situation is similar in $ZnSe/ZnS_xSe_{1-x}$,[4,5] $Zn_xCd_{1-x}S/ZnS$,[6] and $ZnSe/Zn_xMn_{1-x}Se$.[7] To realize ideal quantum confinement in SL's and related devices that will operate in pure blue regions or shorter wavelengths, proper sharing of band offsets among conduction and valence bands is necessary in order to confine both electrons and holes to the well layers.

Recently, we have grown ZnSe/MgS SL's by using proper precursors in metalorganic vapor phase epitaxy (MOVPE).[8] Among the binary compound semiconductors in the blue/green region, the combination of ZnSe and MgS gives the maximum energy gap difference and has lattice constants close to that of GaAs substrates. Although MgS naturally forms the rocksalt structure, growth of zinc-blende ZnSe/MgS SL's on (001) GaAs substrates were identified with high-resolution x-ray diffraction measurements.[9] These zinc-blende ZnSe/MgS SL's were grown coherently to the GaAs substrates up to the total thickness of around 3000 Å by the MOVPE method. Another trial to grow ZnSe/MgS SL's was reported with molecular-beam epitaxy (MBE).[10] They reported that two or three monolayers of MgS was the limit for the zinc-blende MgS growth, while the zinc-blende MgS could be grown up to 50–100 Å in the ZnSe/MgS SL's with the present method.[9]

Figure 1 shows the band diagram expected for the ZnSe/MgS SL. The energy-gap difference up to 1.7 eV will be possible in this heterostructure. If we follow the common anion rule, ZnS and MgS will have the same energy location of the valence band top. Since the conduction-band offset between the common cation systems of ZnSe and ZnS is known to be about 70 meV,[11] band offsets of 0.67 and 1.01 eV are estimated for the conduction band and for the valence band, respectively.[12] These values will be large enough to confine both electrons and holes to the ZnSe well layer. Furthermore, using the lattice constant of 5.59 Å recently determined for the zinc-blende MgS,[9] relatively small lattice mismatch (~1.4%) between ZnSe wells and MgS barriers is possible in this heterostructure. Therefore, from a viewpoint of crystalline quality of grown SL's and carrier confinement to well layers, ZnSe/MgS SL's will be a promising material for investigating excitonic properties. In comparison to

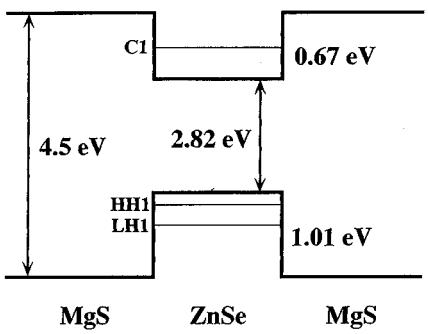

FIG. 1. Band diagram of ZnSe/MgS heterostructure.

$Zn_xCd_{1-x}Se$ and $Zn_xCd_{1-x}S$ wells, ZnSe wells are free from alloy broadening. This will make the discussion on physical phenomena more straightforward.

In this paper, a detailed study on optical properties of ZnSe/MgS SL's is reported. In order to investigate the excitonic properties in these SL's, reflection spectroscopy was used. The advantage of reflection spectroscopy is that reflectance is independent of nonradiative recombinations, therefore the measurements are possible in a wider temperature range in comparison to photoluminescence (PL) and photoluminescence excitation (PLE) spectroscopy, which are based on radiative recombination processes. Furthermore, reflectance measurements do not require the etching process of GaAs substrates, which is usually necessary for measuring absorption spectra. A theoretical fitting method to the measured reflection spectra was developed considering the multiple reflection in the transparent SL films. The exciton absorption peak positions and exciton linewidths were estimated with good accuracy. The prepared ZnSe/MgS SL's showed clear excitonic enhancement and excitonic peaks were clearly observed from 13 K to the measured room temperature. The blueshift of the exciton peaks by the quantum confinement in the ZnSe/MgS SL's is compared with the theoretical calculation. The temperature dependence of the exciton linewidth is also discussed. Since MgS in the barrier layers has higher ionicity than ZnS_xSe_{1-x}, the exciton–LO-phonon coupling in this SL may be enhanced if the wave function is penetrated into the barrier layers for narrow wells and the resultant scattering is enhanced through the Frölich interaction in the barrier layers. On the other hand, the exciton–LO-phonon coupling will be reduced if the quantum confinement effect in narrow wells dominate as is observed in other SL's.[1,2,13] The present measurements show that the latter effect of the quantum confinement dominates in the ZnSe/MgS SL's, and the exciton–LO-phonon coupling is reduced for narrower wells.

II. SAMPLE PREPARATION

ZnSe/MgS strained SL's were grown on semi-insulating GaAs(001) substrates with atmospheric-pressure (AP) MOVPE. For the growth of MgS, bismethyl cyclopentadienyl-magnesium $[(MeCp)_2Mg]$ and di-isopropyl sulfide (DiPS) were selected as precursors. For the growth of ZnSe, di-ethyl zinc (DEZn) and tertiarybutyl isopropyl selenide (tBiPSe) were used. Since the growth of MgS was observed above 450 °C, the growth temperature was set to 450 °C. For the straightforward analysis of the reflection spectra, SL structures were grown directly on GaAs substrates without buffer layers starting from the ZnSe layer. The sample surfaces were terminated with the ZnSe layer for preventing MgS layers from being oxidized. During the growth, the growth rate was monitored *in situ* by an optical multiple reflection in the films with a He-Ne laser (632.8 nm). From this monitoring, the ratio of the ZnSe/MgS layer thickness was measured. Therefore together with the SL period calculated from the SL satellite peaks in x-ray diffraction measurements, the thickness of ZnSe and MgS layers in SL's were determined.[8,9] Characterization of SL's was carried out with optical reflectance and PL measurements. In reflectance measurements, a halogen lamp was used as a light source, and throughout this work, measurements were performed with incident light propagating along the normal to the SL surfaces.

III. CALCULATION OF REFLECTION SPECTRA

To obtain excitonic properties such as absorption peak positions, absorption intensities, and half-widths of absorption peaks from reflection spectra, measured reflection spectra were fitted by a theoretical calculation. In this calculation, exciton absorptions were treated as Lorentzian functions, which are appropriate for the weak exciton-phonon coupling case. The criteria to distinguish the weak and strong coupling cases were fully discussed by Rudin, Reinecke, and Segall[14] and they showed that the most III-V and II-VI materials satisfy the criterion for the weak coupling case. The measured reflection spectra were highly modified by the multiple reflection from all of the epitaxial layers and the optical interference between the lights reflected from the sample surface and from the heterointerface to the GaAs substrate were taken into account. Power reflectivity from the sample surface in the normal incidence arrangement is expressed as follows:

$$R=\frac{(r+r'e^{\alpha L})^2-4rr'e^{\alpha L}\sin^2(\delta/2)}{(1+rr'e^{\alpha L})^2-4rr'e^{\alpha L}\sin^2(\delta/2)}, \tag{1}$$

where r is the amplitude reflectivity from the sample surface to the air, r' is the one from the GaAs heterointerface to the film, α is the absorption coefficient in the film, and δ is the optical path length in the film, which is given by $\delta=4\pi n_{\rm epi}L/\lambda_0$. $n_{\rm epi}$ is the refractive index of the SL, L is the total epitaxial layer thickness, and λ_0 is the wavelength of the incident light.

When excitonic contributions to the refractive index and the absorption coefficient are given explicitly, $n_{\rm epi}$ and α are given by the following equations:[15]

$$n_{\rm epi}=n_0-\sum_i \alpha_i \frac{c}{2\pi\nu}\frac{\Delta_i\Gamma_i}{4\Delta_i^2+\Gamma_i^2}, \tag{2}$$

$$\alpha=\alpha_0+\sum_i \alpha_i \frac{\Gamma_i^2}{4\Delta_i^2+\Gamma_i^2}. \tag{3}$$

n_0 and α_0 are the average refractive index and the absorption coefficient of the SL, respectively, except for the excitonic contribution. i denotes the excitonic states, c is the light velocity, α_i is the line center absorption coefficient of the ith exciton state. $\Delta_i=\nu-\nu_{i0}$ and ν_{i0} defines the peak position of the exciton absorption. Γ_i is the full width at half maximum (FWHM) of exciton absorption. The amplitude reflectivity r and r' are calculated using the refractive indices of the epitaxial layer $n_{\rm epi}$ and of the substrate n_s with the form of $r=(n_{\rm epi}-1)^2/(n_{\rm epi}+1)^2$, $r'=(n_s-n_{\rm epi})^2/(n_s+n_{\rm epi})^2$.

Figure 2 shows illustrative reflection spectra obtained by the theoretical calculation, showing the variation of the excitonic features depending on the exciton peak position relative to the multiple reflection spectra. In these examples, total epitaxial layer thickness is given as 1700 Å, and the exciton absorption peak wavelength $\lambda_{i0}(=c/\nu_{i0})$ is assumed to be at (a) 440 nm, (b) 500 nm, (c) 555 nm, and (d) 620 nm for illustrative purposes. The slowly varying structures com-

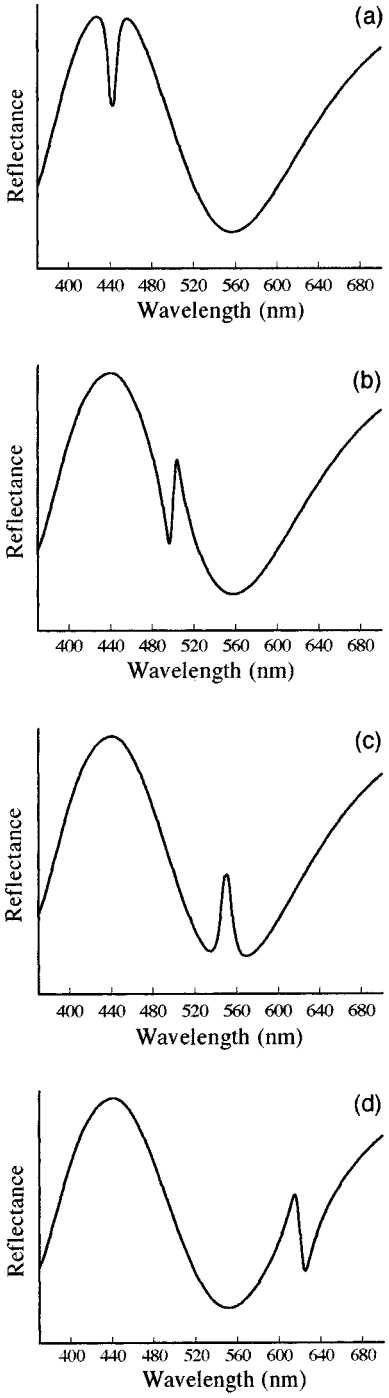

FIG. 2. Illustrative reflection spectra calculated for a ZnSe/MgS SL with the 1700-Å total thickness on GaAs. The exciton peak position was hypothetically assumed to be at (a) 440 nm, (b) 500 nm, (c) 555 nm, and (d) 620 nm to show the change of the exciton features by the position relative to the multiple reflection in the film.

mon in the four cases are caused by multiple reflection. Fitting to this multiple reflection spectrum gives us the total epitaxial layer thickness with the knowledge of the refractive index. The sharp structures superimposed on the multiple reflection spectra are the excitonic contributions. It is much different depending on the exciton peak positions. When the exciton peak is located near the top or bottom of the multiple reflection spectra, a single peak appeared as shown in Figs. 2(a) and 2(c). These exciton spectra are similar to the results

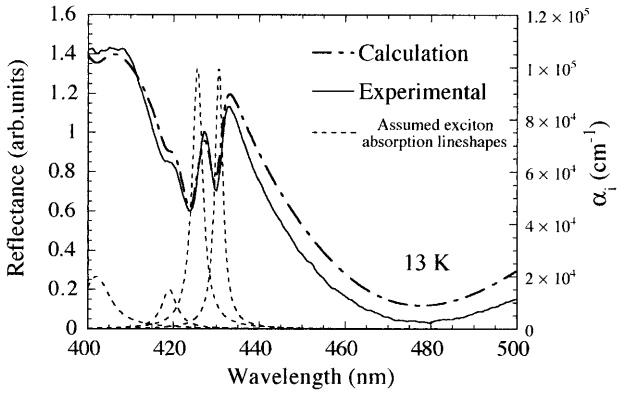

FIG. 3. Reflection spectrum measured on a ZnSe/MgS SL on GaAs (solid line) and its theoretical fit (dot-dashed line). The four peaks (dashed lines) are the exciton absorptions assumed for the theoretical fit.

derived with the single-path reflection model,[16,17] where only the interference between the reflection from the surface and the single-path reflection from multiple quantum wells (MQW) was considered. Following this model, the exciton spectra reflect the real or imaginary part of the exciton dielectric constants depending on the phase shift by the path length between the surface and the MQW layers. In the present case, the phase shifts at the maximum and minimum multiple reflections select the imaginary part of the exciton dielectric constant as shown in Figs. 2(a) and 2(c). In the two cases, the polarity of the excitonic contribution is opposite depending on the phase shift of the multiple reflection. At the middle level of the multiple reflections, the real part of the exciton dielectric constant dominates in the reflection spectra as shown in Figs. 2(b) and 2(d), by the phase shift from the multiple reflection similar to the above cases of Figs. 2(a) and 2(c). Since the real part of the excitonic refractive index is antisymmetric, the excitonic contribution in Figs. 2(b) and 2(d) are also asymmetric.

In the actual calculation, which will be discussed in the next section, the reflections at the sample surface and the interface to the GaAs substrate were taken into account, but the smaller reflections at the SL heterointerfaces were neglected for simplicity. The refractive index dispersion relations of ZnSe and MgS were obtained by a modified single effective oscillator model.[17–20] The average refractive index of the SL layer n_0 was approximated by the mean value of the two layers weighted with the respective thicknesses.

IV. RESULTS AND DISCUSSIONS

The experimentally measured reflection spectrum (solid line) was compared with the result of theoretical calculation (dot-dashed line) in Fig. 3. The sample structure measured is the SL with 18 periods of 54-Å-thick ZnSe well layers and 24-Å-thick MgS barrier layers. Measurements were carried out at 13 K. The slowly varying feature in the measured spectrum is due to the multiple reflection. The clear structures around 430 nm due to excitonic effects are evident. The measured reflection spectrum was nicely reproduced by the theoretical fitting shown by the dotted-dashed line in Fig. 3. The accuracy of this fitting method depends on the sharpness of the excitonic features and the sharpness was good enough even at room temperature. For this fitting, we had to include

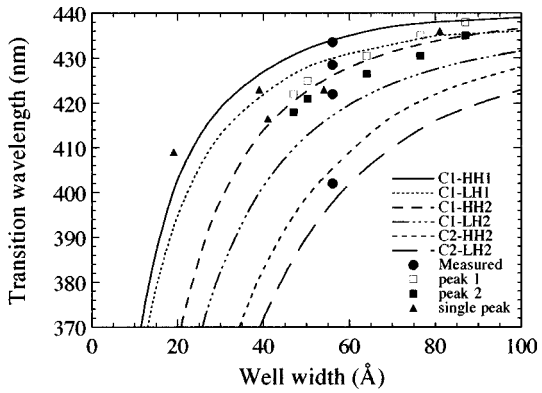

FIG. 4. Comparison of exciton peaks measured in Fig. 3 (closed circles) and calculated transition wavelength between subbands. Well width dependence of other measured $C1$-HH1 and $C1$-LH1 exciton peaks are also plotted (open and closed squares). In some SL samples, the separation of the $C1$-HH1 and $C1$-LH1 peaks was not clear (closed triangles). The energy separations of the two peaks shown by the open and closed squares were in reasonable agreement with the calculation.

four excitonic peaks that are clear in the measured reflection spectrum in the 400–440-nm range from the deviation from the normal multiple reflection spectrum. The dashed lines are the assumed exciton absorption peaks with the Lorentzian line shapes given by the second term in Eq. (3). The α_i values fitted for the major two peaks are 100 000 cm^{-1} at 13 K in Fig. 3. To identify the origin of each exciton peak, the peak positions determined from the fitting were compared with the calculated transition wavelength.

Figure 4 shows the theoretical calculation of the transition wavelength between subbands. The excitonic absorption peak positions determined in Fig. 3 are shown by the solid circles. Parameters used in this calculation were listed in Table I. Since zinc-blende MgS did not exist before, no measured effective masses for MgS were available and the effective masses of the same sulfide, ZnS, were assumed in Table I. The influence of the barrier effective masses on the calculated subband energies was numerically checked. Since the band offsets discussed in Ref. 12 are rather large in the two models, calculated subband energies are rather insensitive to the MgS effective masses and also on the band offsets. In this calculation of the transition wavelength, exciton binding energies and strain effects were also included. Exciton binding energies were calculated by a variational method, where an anisotropic trial wave function for the exciton relative motion was used with two variational parameters.[21] The heavy-hole (HH) exciton binding energies in the ZnSe/MgS SL's were calculated to be 32 meV for the 54-Å ZnSe well and increased further for the narrower wells. Since the difference of the exciton binding energies between HH and light-hole (LH) excitons is not large except for very narrow wells,[22] LH exciton binding energies were assumed to be the same as the HH excitons in Fig. 4 for simplicity.

TABLE I. Parameters used in subband transition calculation. Parameters for ZnSe were taken from Ref. 4. Effective masses for zinc-blende MgS are not yet known and were assumed to be the same as ZnS. (effective masses are in the unit of m_0, C_{ij}'s are 10^6 kg cm^{-2})

	a_0 (Å)	E_g (eV)	$m^*(C)$	m^*(HH)	m^*(LH)
ZnSe	5.669	2.82	0.147	0.6	0.31
MgS	5.59	4.5	0.27	0.49	0.49
	C_{11}	C_{12}	a (eV)	b (eV)	
ZnSe	0.826	0.498	5.40	1.2	

Since the present ZnSe/MgS SL's with the relatively thin total layer thicknesses less than 2000 Å are grown coherently on (001) GaAs substrates, the in-plane lattice constants of the SL's $a_{\parallel}$ will be equal to that of GaAs. Then the strain in the ZnSe well layer is given by $\epsilon=(a_{\parallel}-a_{\mathrm{ZnSe}})/a_{\mathrm{ZnSe}}$ (we defined the strain to be positive for tensile strain). Since the lattice constant of ZnSe is larger than that of GaAs and MgS, ZnSe well layers are subject to compressive stress. The energy shifts induced by the strain relative to the conduction-band edge at the Γ point are given by Ref. 23, and they are simplified in the following forms under the condition of $\Delta \gg E_U$:

$$\Delta E_{\mathrm{HH}}=-E_H+E_U, \tag{4a}$$

$$\Delta E_{\mathrm{LH}}=-E_H-E_U, \tag{4b}$$

where $E_H=2a(1-C_{12}/C_{11})\epsilon$ and $E_U=b(1+2C_{12}/C_{11})\epsilon$. Δ is the spin-orbit split-off energy. The parameter a is the hydrostatic deformation potential, b is the shear deformation potential, and C_{ij}'s are the elastic stiffness constants. The HH-LH band splitting of $2E_U$ induced by the compressive strain in the well layer is estimated to be $\sim$15 meV. This E_U value is much smaller than the Δ value in ZnSe, which is 430 meV. Since the lattice mismatch between ZnSe and GaAs is small ($\sim$0.3%), the strain-induced modification of the band offsets in the present SL's grown coherently on GaAs substrates is at most 20 meV. This is much smaller than the band offsets shown in Fig. 1, and the strain-induced modification of the band offsets will be negligible.

From the comparison of the measured exciton peak positions and the calculated transition energies, the two major exciton peaks in Fig. 3 were identified as the $C1$-HH1 and $C1$-LH1 exciton transitions. The third small exciton contribution is close to the $C1$-HH2 transition. The transition between the $C1$ and HH2 subbands is normally forbidden because of the parity selection rule. The observation of the weak $C1$-HH2 transition suggests that there remains slight asymmetry in the grown SL. The most probable factor will be tailing of the grown ZnSe/MgS heterointerfaces due to the inadequate gas exchange during the MOVPE growth. The fourth exciton peak in the shorter wavelength is most probably the contribution from the $C2$-HH2 transition, but the additional contribution from the $C2$-LH2 transition may be superimposed. In Fig. 3, intensity of the $C1$-LH1 exciton absorption peak is comparable to that of the $C1$-HH1 peak. In the present reflectance measurements, the electric field of the incident light is polarized parallel to the well layers. The observed large contribution of the $C1$-LH1 exciton is different from the normally predicted oscillator strength ratio of 3 to 1 for C-HH and C-LH transitions, respectively.[24] Detailed discussion on this point needs further experimental studies.

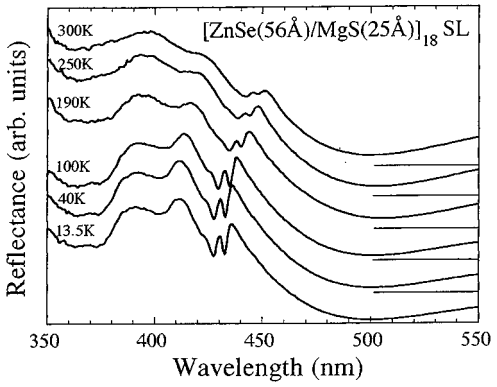

FIG. 5. Temperature dependence of reflection spectra measured on a ZnSe/MgS SL. The $C1$-HH1 and $C1$-LH1 excitonic structures around 440 nm were clearly visible up to room temperature.

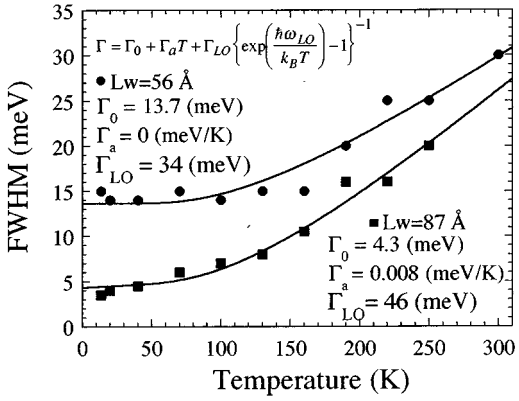

FIG. 6. Temperature dependence of FWHM of $C1$-HH1 exciton absorption line shape measured on two ZnSe/MgS SL's. For the 56-Å-thick ZnSe wells, the inhomogeneous broadening of 13.7 meV and the LO-phonon coupling constant of 34 meV were obtained with the fitting. For the 87-Å-thick ZnSe wells, the inhomogeneous broadening of 4.3 meV and the LO-phonon coupling constant of 46 meV were obtained with the fitting.

The well-width dependence of the absorption peak wavelengths extracted from the reflection spectra on other SL's is also shown in Fig. 4. In this figure, the measured exciton peaks related to $C1$-HH1 and $C1$-LH1 were plotted with open and closed squares, respectively. Some samples showed only one peak in the corresponding range as shown by closed triangles, maybe because of poor interface properties. The blueshift of the measured exciton peaks for the narrower well widths is in accordance with the calculated transition wavelength. Although the measured exciton peaks show the tendency to shift to shorter wavelengths than the calculated ones, the separations of the two exciton peaks are very close to the calculated HH1-LH1 separations. The tendency that the measured transition wavelengths are slightly shifted to shorter wavelength than the calculated ones is not due to the theoretical fitting method but is due to the problem remaining in the growth of the superlattices. Especially, there remains the problem of extra MgSe layer formation with the thickness of less than 1 ML at the interfaces depending on how the interfaces were grown.[25] Clear excitonic features are not observed in these SL's with the extra MgSe layers and the details are under study.

In order to investigate the excitonic effects in the ZnSe/MgS SL's at the higher temperature, the temperature dependence of the reflection spectrum was measured as shown in Fig. 5. The measured sample is the SL with 18 periods of ZnSe(56 Å)/MgS(25 Å). It is noted that the $C1$-HH1 and $C1$-LH1 excitonic structures around 440 nm remain clearly visible up to room temperature. This will demonstrate the enhanced excitonic effect due to the quantum confinement in this SL. From these measurements, the temperature dependence of the FWHM of the exciton absorption line shape can be discussed. It is interesting to investigate the exciton–LO-phonon coupling in the ZnSe/MgS system from the measured exciton linewidth. The reduction of the exciton–LO-phonon coupling was reported on $Zn_xCd_{1-x}Se$/ZnSe QW's (Refs. 1, 2, and 26) and on CdTe/$Zn_xCd_{1-x}Te$ QW's (Ref. 27) with quantum confinement effect, while the FWHM LO-phonon coupling parameter Γ_{LO} of the exciton linewidth in ZnSe/ZnS SL's (Refs. 28 and 29) and in ZnSe/ZnS_xSe_{1-x} SL's (Ref. 30) was similar to the bulk ZnSe value of 60 meV.[29] This will be because of the small conduction-band offsets in the ZnSe/ZnS_xSe_{1-x} and ZnSe/ZnS SL's and the resultant weak quantum confinement.

Because of the high ionicity in the MgS barrier layers in the present SL's, the exciton–LO-phonon coupling will be enhanced if the Frölich interaction in the barrier layer is dominant. For example, Cd-related compounds have higher ionicity and the exciton linewidth measured in $Zn_xCd_{1-x}Se$/ZnSe quantum wells increased for the higher Cd content for the fixed well width of 3 nm.[2] This was attributed to the increased exciton-phonon coupling in $Zn_xCd_{1-x}Se$ wells with higher Cd content. Therefore, it is not very clear whether the LO-phonon coupling parameter Γ_{LO} decreases in the ZnSe/MgS SL's when the well thickness gets thinner. There may be competition between the exciton quantum confinement effect and the enhancement of exciton-phonon scattering due to the increased penetration of the wave functions to MgS barrier layers when well layers get thinner. Two SL samples with the well widths of 56 and 87 Å were examined on FWHM of the $C1$-HH1 exciton absorption line shape, and the results are shown in Fig. 6. The closed circles and squares are the measured FWHM in the respective SL's with the well width of 56 and 87 Å. The solid lines are fitting with the inhomogeneous broadening Γ_0, acoustic phonon scattering, and the exciton–LO-phonon scattering. The deviation of the measured data from the fitted line is a measure of the accuracy in the line-shape fitting discussed in Sec. III. The deviation is within 1–2 meV. For the well width of 56 Å, the measured values are almost constant up to 100 K and the acoustic phonon scattering, which is proportional to the temperature and is usually dominant in the low-temperature range, was neglected. The exciton–LO-phonon coupling parameter Γ_{LO} was estimated to be 34 meV for the SL with the 56-Å well. For the SL with the 87-Å well, the measured FWHM value showed the higher temperature dependence in the low-temperature range than that of the SL with the 56-Å well. Therefore the acoustic-phonon scattering term was included and the nice fitting shown with the solid line was obtained with the parameters given in Fig. 6. The Γ_{LO} value of 46 meV thus determined in Fig. 6, however, will have the uncertainty of ± 3 meV because of the increased fitting parameters.

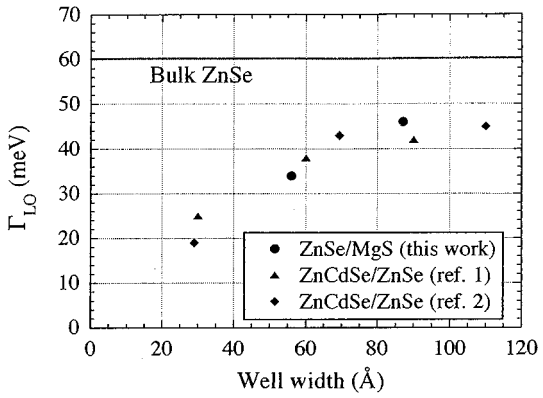

FIG. 7. LO-phonon coupling constant derived in the present ZnSe/MgS SL's was compared with that reported in $Zn_xCd_{1-x}Se/ZnSe$ SL's. All the constants were reduced compared with the bulk ZnSe value.

Our results on Γ_{LO} were compared in Fig. 7 with the $Zn_xCd_{1-x}Se/ZnSe$ system that was reported in Refs. 1 and 2. All the measured values in Fig. 7 were smaller than the bulk value of about 60 meV in ZnSe. The Γ_{LO} values measured in the present ZnSe/MgS SL's were reduced for the narrower wells and were close to those measured in $Zn_xCd_{1-x}Se/ZnSe$ QW's. This shows that the MgS barriers with high ionicity do not play essential roles in the exciton–LO-phonon scattering in the measured ZnSe/MgS SL's. From this result, we can conclude that the penetration of the exciton wave functions is not significant and the quantum confinement effect on excitons dominates. Further measurements on SL's with the well width less than 60 Å will be interesting from two aspects. One point is that the exciton quantum confinement increases for this range of well widths that is less than the bulk exciton Bohr diameter of ZnSe. The large band offsets in the ZnSe/MgS SL's may results in the further reduction of the exciton–LO-phonon coupling compared to other II-VI SL's. The other point is that the penetration of the wave functions will increase for the narrow well region that may increase the LO-phonon coupling. At present, the inhomogeneous broadening in the narrow well region is too large to accurately estimate the exciton linewidth. Further improvement of the heterointerfaces in the grown ZnSe/MgS is necessary and the study is under progress.

V. CONCLUSIONS

Excitonic properties in the ZnSe/MgS SL's were examined. We showed that reflectance measurement is a useful method to investigate optical properties by employing the fitting with the developed simulation. It is free from substrate removal and the optical properties at room temperature can be easily studied. Excitonic parameters such as absorption peak positions, absorption intensities, and half widths were obtained by employing the Lorentzian exciton line-shape function assumed in the theoretical simulation. The exciton absorption peak positions determined from the reflection spectra agreed well with the subband transition wavelength calculated. Up to room temperature, excitonic structures were clearly observed. This result strongly indicates the enhancement of the exciton effects in ZnSe/MgS SL's. Reduction of the exciton–LO-phonon coupling constant was clearly observed for excitons in narrower wells.

ACKNOWLEDGMENTS

This work was supported in part by the Grant-in-Aid for Scientific Research from the Ministry of Education, Science and Culture, No. 07455126.

*Author to whom correspondence should be addressed.

[1] N. T. Pelekanos, J. Ding, M. Hagerott, A. V. Nurmikko, H. Luo, N. Samarth, and J. K. Furdyna, Phys. Rev. B **45**, 6037 (1992).

[2] R. Cingolani, P. Prete, D. Greco, P. V. Giugno, M. Lomascolo, R. Rinaldi, L. Calcagnile, L. Vanzetti, L. Sorba, and A. Franciosi, Phys. Rev. B **51**, 5176 (1995).

[3] J. S. Massa, G. S. Buller, A. C. Walker, G. Horsburgh, J. T. Mullins, K. A. Prior, and B. C. Cavenett, Appl. Phys. Lett. **66**, 1346 (1995).

[4] K. Shahzad, D. J. Olego, and C. G. Van de Walle, Phys. Rev. B **38**, 1417 (1988).

[5] Y. Kuroda, I. Suemune, M. Fujimoto, Y. Fujii, N. Otsuka, and Y. Nakamura, J. Appl. Phys. **72**, 3029 (1992).

[6] T. Taguchi, C. Onodera, Y. Yamada, and Y. Masumoto, Jpn. J. Appl. Phys. **32**, L1308 (1993).

[7] R. B. Bylsma, W. M. Becker, T. C. Bonsett, L. A. Kolodziejski, R. L. Gunshor, M. Yamanishi, and S. Datta, Appl. Phys. Lett. **47**, 1039 (1985).

[8] T. Obinata, H. Kumano, K. Uesugi, J. Nakahara, and I. Suemune, *Extended Abstracts of 1995 International Conference on Solid State Devices and Materials* (Business Center for Academic Societies, Japan, 1995), p. 1091.

[9] K. Uesugi, T. Obinata, H. Kumano, J. Nakahara, and I. Suemune, Appl. Phys. Lett. **68**, 844 (1996).

[10] N. Teraguchi, H. Mouri, Y. Tomomura, A. Suzuki, H. Taniguchi, J. Rorison, and G. Duggan, Appl. Phys. Lett. **67**, 2945 (1995).

[11] Y. Yamada, Y. Masumoto, and T. Taguchi, Phys. Rev. B **44**, 4 (1991); **44**, 1801 (1991).

[12] In comparison to 0.67 and 1.01 eV for the conduction and valence bands, respectively, estimated from this simple common anion rule, the tight-binding Harrison model predicts 1.02 and 0.66 eV for the conduction and valence bands, respectively. There also remains the possibility of modification of these values by the consideration of the *d* orbitals of cation atoms in addition to the strain effect.

[13] N. T. Pelekanos, H. Haas, N. Magnea, H. Mariette, and A. Wasiela, Appl. Phys. Lett. **61**, 3154 (1992).

[14] S. Rudin, T. L. Reinecke, and B. Segall, Phys. Rev. B **42**, 11 218 (1990).

[15] Y. Zhu, D. J. Gauthier, S. E. Morin, Q. Wu, H. J. Carmichael, and T. W. Mossberg, Phys. Rev. Lett. **64**, 2499 (1990).

[16] X. L. Zheng, D. Heiman, B. Lax, and F. A. Chambers, Appl. Phys. Lett. **52**, 287 (1988).

[17] B. Zhang, S. S. Kano, Y. Shiraki, and R. Ito, Phys. Rev. B **50**, 7499 (1994).

[18] S. H. Wemple and M. D. DiDomenico, Phys. Rev. B **3**, 1338 (1971).

[19] M. A. Afromowitz, Solid State Commun. **15**, 59 (1974).

[20] The values for the parameters E_0, Eg, and E_d in the formula

given in Ref. 19 are given in Ref. 18 for ZnSe. The parameters for MgS were given as follows: E_0=7.5 eV (extrapolated from the energy gap dependence in other II-VI semiconductors), Eg =4.5 eV (energy gap of MgS) and E_d=27 eV (almost the common value among the similar II-VI semiconductors).

[21] I. Suemune (unpublished).

[22] P. Christol, P. Lefebvre, and H. Mathieu, J. Appl. Phys. **74**, 5626 (1993).

[23] F. H. Pollak and M. Cardona, Phys. Rev. **172**, 816 (1968).

[24] M. Yamanishi and I. Suemune, Jpn. J. Appl. Phys. **23**, L35 (1983).

[25] H. Suzuki, T. Obinata, H. Nashiki, H. Kumano, K. Uesugi, I. Suemune, and J. Nakahara, *Extended Abstracts of 43rd Spring Meeting, 1996* (Japan Society of Applied Physics, Tokyo, 1996), p. 266.

[26] P. M. Young, E. Runge, M. Ziegler, and H. Ehrenreich, Phys. Rev. B **49**, 7424 (1994).

[27] N. T. Pelekanos, H. Haas, N. Magnea, H. Mariette, and A. Wasiela, Appl. Phys. Lett. **61**, 3154 (1992).

[28] Y. Kawakami and T. Taguchi, J. Vac. Sci. Technol. B **7**, 789 (1989).

[29] F. Yang, P. J. Parbrook, B. Henderson, K. P. O'Donnell, P. J. Wright, and B. Cockayne, Appl. Phys. Lett. **59**, 2142 (1991).

[30] M. Dabbicco, G. Scamarcio, V. Spagnolo, R. Tommasi, M. Lugara, M. Ferrara, I. M. Catalano, R. Cingolani, M. Lomascolo, C. Stevens, R. Taylor, J. Ryan, I. Suemune, and Y. Kuroda, *Advances in Science and Technology 11*, edited by P. Vincenzini and G. C. Righini (Techna Srl, Rome, 1995), p. 331.